African Journal of Environmental Science and Technology

AJ ACADEMIC JOURNALS
expand your knowledge

Full Length Research Paper

Modelling and simulation of atmospheric conditions impact on photovoltaic production in Saint Louis area

Abdoulaye Bouya DIOP[1*], Bouya DIOP[1], Abdou Karim FAROTA[1], Ababacar THIAM[2], Aichetou DIA[1] and Djiby SARR[1]

[1]Atmosphere and Oceans Sciences Laboratory, Gaston Berger University, Senegal.
[2]Department of Mathematical, Aliou SOW University of Bambey, Senegal.

In this study, we worked on the modelling and the simulation of atmospheric conditions impact on photovoltaic production in Saint Louis area. Using Ineichen's model based on the disorder factor of Link, an assessment of sunshine in the study area was made. A characterization of the irradiation is elaborated by modelling the radiation and by simulating outputs of a photovoltaic power plant. We can estimate aerosols impact on photovoltaic production in the river area thanks to results obtained. We evaluated the sunshine rate of this area by using the modelling process. We chose an irradiation model to estimate the outputs of a photovoltaic power plant subjected to an atmosphere disturbed by aerosols. This work enabled us to set up a system of alerts and specific warnings for populations benefiting from this type of resource.

Key words: Photovoltaic output, atmosphere, aerosol, sunshine, alert, Saint Louis area.

INTRODUCTION

In Saint Louis, the atmosphere is influenced by desert dust (D'Almeida 1986). This Sahelian area near Sahara Desert is a climatic area, which is subjected throughout the year to dust episodes (Kaly, 2015). During the rainy season, heavy clouds appear which unfortunately produce few rains (Chamani et al., 2018) and can disturb the area insolation. During the dry season, Saint Louis area is exposed to dust occurrences. These dust occurrences in most cases are mineral aerosols commonly called "desert dust", have a very marked seasonal cycle and whose timing coincides partially with that of Harmattan (Martiny et al., 2016). Thus, if the dry season extends from October to March, we can distinguish a period "without" dust from July to December and a period "with" dust from January to June. The latter can be split into two sub-periods: from January to March and from April to June (Martiny et al., 2016). It is in the dry season that the continental trade winds in the North / Northeast direction speed increase in the lower atmospheric layers and bring with them significant amounts of desert dust from the Sahara to the Sahel (Senghor, 2017).

With the advent of photovoltaic energy and the urgent need to control global warming (Arent et al., 2011)

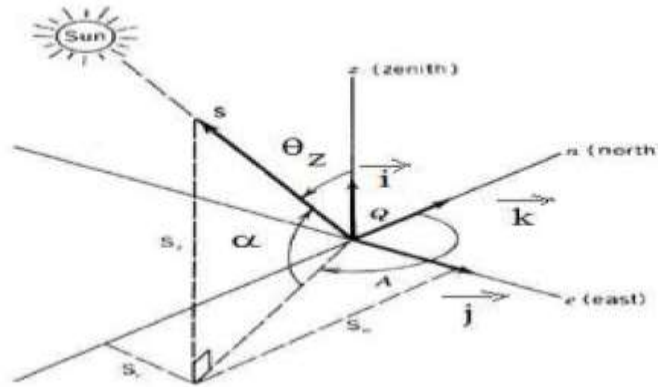*Corresponding author. E-mail: bouya.diop@ugb.edu.sn.

Figure 1. Horizontal coordinates system for the S position vector identified by the coordinates α, θz et A.

power plants are being created everywhere (Laines-Canepa et al., 2017), including in Saint-Louis area, with the 20-megawatt solar center of Bokhol (Maillard, 2017).

However, a major problem remains with the use of photovoltaic energy. This technology uses solar radiation to produce energy (Gratzel, 2005). These radiations must cross the atmosphere before reaching the sensor. Saint Louis area is an area with high concentration of dust and cloud cover more or less important depending on the period of year and seasons. This radiation will necessarily be subject to disturbances (Dickinson 1975) that have been discussed in this work.

So the objective of this work was to correlate the impact of certain atmospheric conditions, notably aerosols and the variability of photovoltaic production in Saint Louis.

MATERIALS AND METHODS

According to the Bouguer-Lambert law, better known as Beer's Law, the attenuation of light through a medium is proportional to the distance covered in the medium and the radiation flux where k is an attenuation coefficient (Abitan et al., 2008).

$$I_{Bn} = I_0 \exp(-kx) \tag{1}$$

Where, I_{Bn} is the radiation attenuated; I_0: is the incidental radiation; K is the attenuation coefficient; x: is the covered distance.

The diversity and multiplicity of radiation prediction methods require a critical look at the accuracy, the performance and even the validity of some models.

It is for this reason that we studied a model proposed in the literature, which is the model of Ineichen (Ineichen, 1992; Kasten 1996) based on disorder factor of Link.

Several models of direct radiation determination based on disorder factor of Link are mentioned in the literature. The difference between these models lies in the factor approach and / or in the formulation of direct solar radiation. This factor is used to characterize the atmospheric disturbance caused by water vapor, mist, fumes, dust, etc. The advantage of these models is that factors attenuating radiation are given according to a single easy-to-use index. For this model, the direct solar radiation is given by Bouhadda and Serrir (2006):

$$I_b = I_0 \exp\left(-\frac{T_L}{0.9 + 9.4 \sin\alpha}\right) \tag{2}$$

Where I_b is the direct solar radiation; I_0 is the incidental radiation and α is the solar height that is the angle between the star and the horizontal plane (Figure 1). As an alternative, the altitude of the sun can be described in terms of the zenithal solar angle θz which is simply the complement of the solar elevation angle,

$$\theta_z = 90° - \alpha (degrees) \tag{3}$$

$$\sin\alpha = \sin\sigma\sin\phi + \cos\phi\cos\omega\sin\phi \tag{4}$$

Where ϕ is the latitude of the place to study; ω is the hour angle is the angular distance between the meridian of the observer and the meridian whose plane contains the sun. This measurement is made from the South turning towards the West.
T_L is the the disorder of Link coefficient is expressed by (5):

$$T_L = 2.4 + 14.6\beta + 0.4(1 + 2\beta)\ln(P_v) \tag{5}$$

With β as the Angström coefficient that expresses the amount of aerosol in the atmosphere; P_v is the atmospheric pressure of the place; σ is the declination. It represents the angle between the sun direction and the equatorial plane. It varies throughout the year (Figure 2).
It is given by the relation (6):

$$\sigma = 23.45\sin\left[\frac{360}{365}(284 + d)\right] \tag{Figure 3} \tag{6}$$

$$\omega = 15(TSV - 12) \tag{7}$$

With TSV as the True solar time is defined in relation to the sun.

$$TSV = TSM + ET/60 \tag{8}$$

ET is the equation of time which is the gap between the TSV and the TSM is called the time equation. Indeed, the variation of the earth speed on its trajectory around the sun introduces a corrective term called noted equation of time:
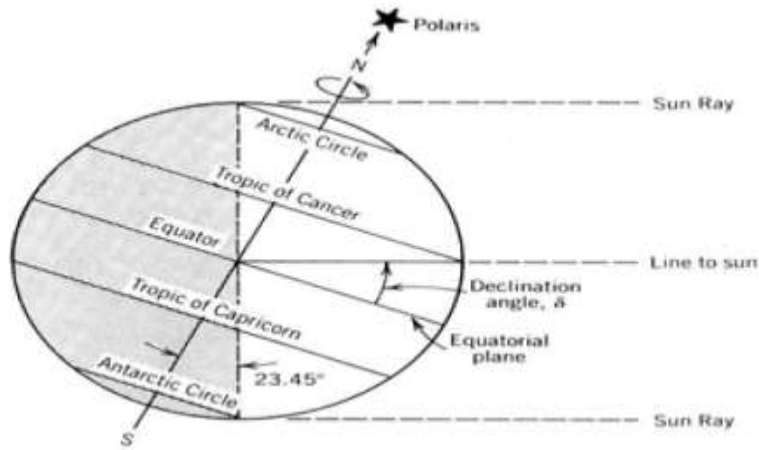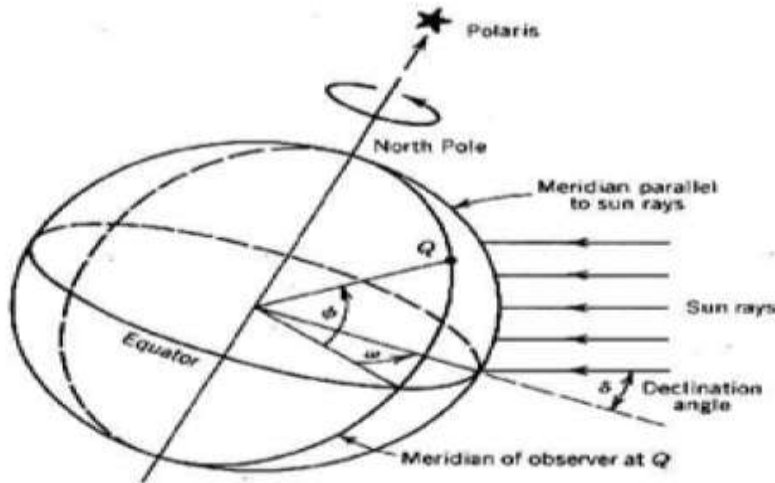
Figure 2. The declination.

Figure 3. The hour angle.

ET=9,9sin [2(0,986d+ 100)] − 7,7sin (0,986d − 2)   (9)

TSM is the mean solar time.

$$TSM = TU + \frac{\lambda_{greenwich} - \lambda}{15}$$ (10)

$\lambda_{greenwich} = 0$

TU s the universal time is the mean solar time of Greenwich. The mean solar time of a longitude location λ (counted in positive numbers towards the west) is related to universal time by Equation (11):

$$TU = TFH + \frac{\lambda_{st}}{15}$$ (11)

TFH is the time zone is an area of the earth's surface within 2 meridians 15° longitude distant.

The time for the TFH time zone is the mean solar time of the reference meridian (of longitude λ_{st}) located in the center of the spindle.

TFH= TL – C   (12)

TL is the legal time TL in a state is usually the time of the time zone but it may differ for convenience and C varies according to the country. In Senegal, C equals zero.

In this study, a modelling of the irradiation has been done by varying the Angström coefficient which expresses the quantity of aerosol in percentage from 0 to 1 in steps of 0.05.

A photovoltaic cell is modelled by the electrical diagram made up of a current generator Isc, a diode D1 and two resistors (shunt Rsh and series) (Edouard and Njomo, 2013).

We modelled the physical model on LT Space, and in a second time we included that physical model in a behavioral model to assign it the irradiation input values obtained by varying the Angström coefficient for the model of Ineichen and by collecting the output voltage of the current or the power received by a possible
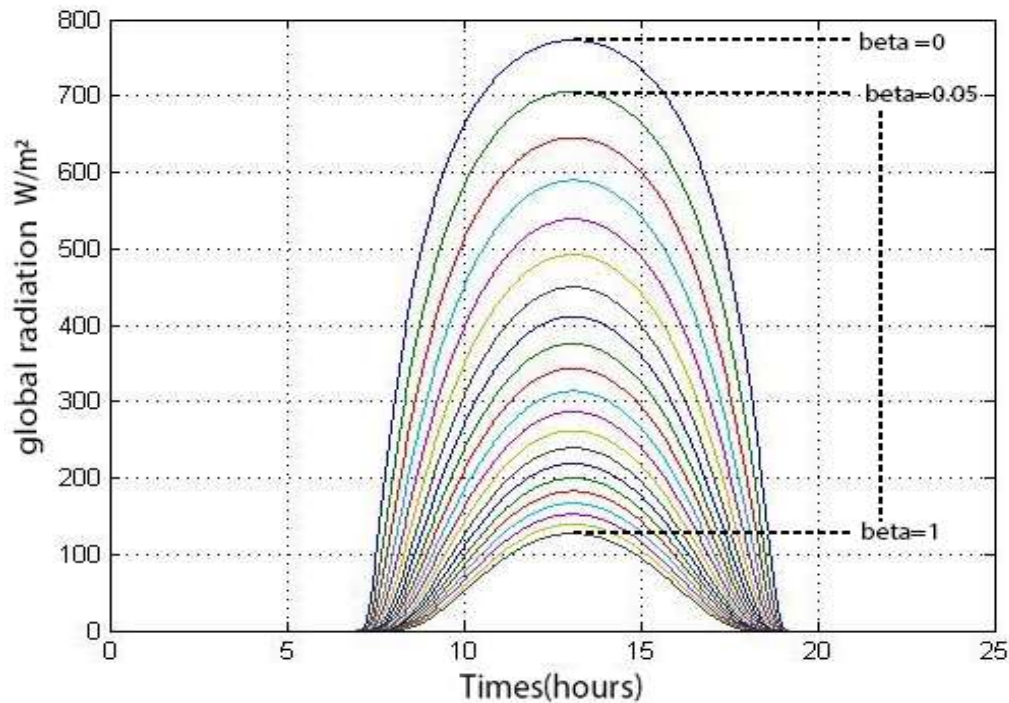
Figure 4. Global radiation variation as a function of time for beta from 0 to 1 in steps of 0.05.

load.

RESULTS

After doing the modelling on Matlab by varying the Angström coefficient which expresses the quantity of aerosols in percentage from 0 to 1 in steps of 0.05, we have the variation of the global radiation as a function of the Angström beta coefficient (Figure 4).

Figure 4 shows the variation of the radiation power as a function of time for different Angström coefficients. We find that the maximum radiation for a beta equals zero and the order is 772.8525W / m^2. The minimum value of the radiation is 127.2792 W / m^2 for a beta equals one (Dyer and Hicks, 1965).

These maximum and minimum values given in Figure 4 are obtained at around 12 Am.

Table 1 gives us the variation of the global radiation max as a function of the Angström beta coefficient. We notice in this table that there are strong values for weak coefficients.

Figure 5 reflects the variation of the maximum radiation as a function of the Angström coefficient. There is a decrease in the maximum power as a function of beta.

Figure 6 reflects a photovoltaic cell. That cell is modelled by the electrical diagram made up of a current generator Isc, a diode D1 and two resistors (shunt Rsh and sériers).

This physical model is in a second time included in a physical model to assign it values of irradiation inputs and temperature, as well as to collect the voltage output of the current or the power received by a possible load.

Figures 7 and 8 show the curves obtained from the simulation of different values of angström beta coefficient.

In the abscissa, there is the duration of the day. In ordinate, there are the powers in Impp (maximum power current) and in Vmpp (maximum power voltage). Note that the maximum power is obtained at about 12 Am and the voltage as well as the current is in phase opposition.

Figures 7a and 8a which show the current evolution indicate the beginning of the current growth at about 7 Am. We noticed that around 6 Pm we have a near zero current.

In Figures 7b and 8b, there was a decrease from 7 Am with a minimum at about 12 Am.

For Figures 7.c and 8.c, the maximum power is obtained at about 12 Am and the voltage as well as the current is in phase opposition.

Similar phenomenon occurs for beta and for all other Beta values. Figure 9 shows for a cell of 10 cm^2 the outcome variation as a function of beta. We notice that there are outcomes higher than 0.7 for beta less than 0.05.

There is outcome decrease. It seems normal that the atmosphere is milder with a high beta.

From this point, an operation mode of the photovoltaic cell is drawn as a function of the aerosol quantity in the

Table 1. Variation of the global radiation max as a function of the Angström beta coefficient.

Beta	0	0.05	0.1	0.15	0.2		0.25	
IB max (W/m²)	772.8525	706.2032	645.3015	589.65196	538.8015		492.3363	
Beta	3	3.35	0.4	0.45	0.5	0.55	0.6	
IB max (W/m²)	449.8781	411.0815	375.6306	343.2369	313.6368	286.5894	261.8744	
Beta	0.65	0.7	0.75	0.8	0.85	0.9	0.95	1
IB max (W/m²)	239.2909	218.6549	199.7985	182.5683	166.8239	152.4373	139.2914	127.2792
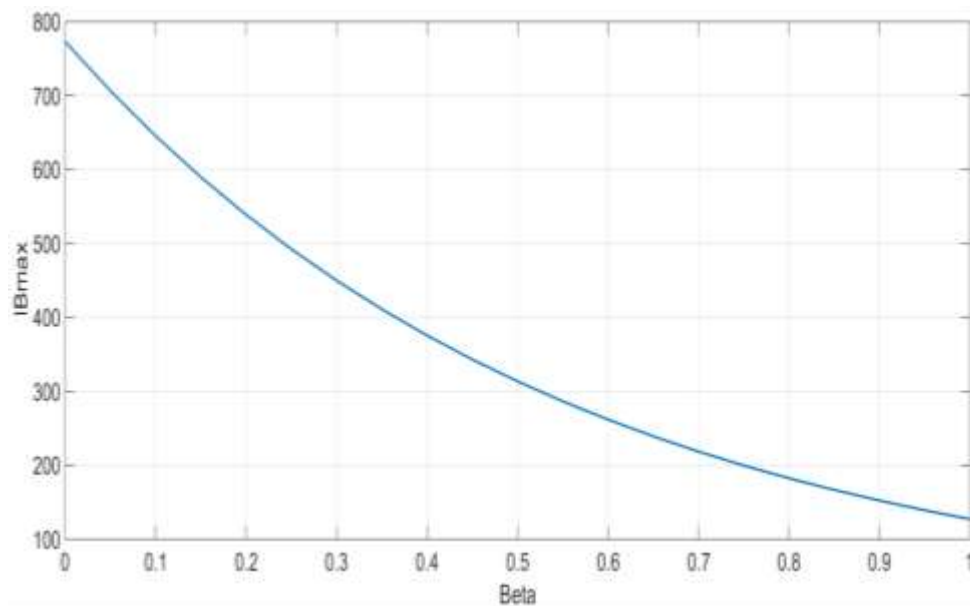
Figure 5. Curve of variation of the global radiation max as a function of the Angström coefficient.
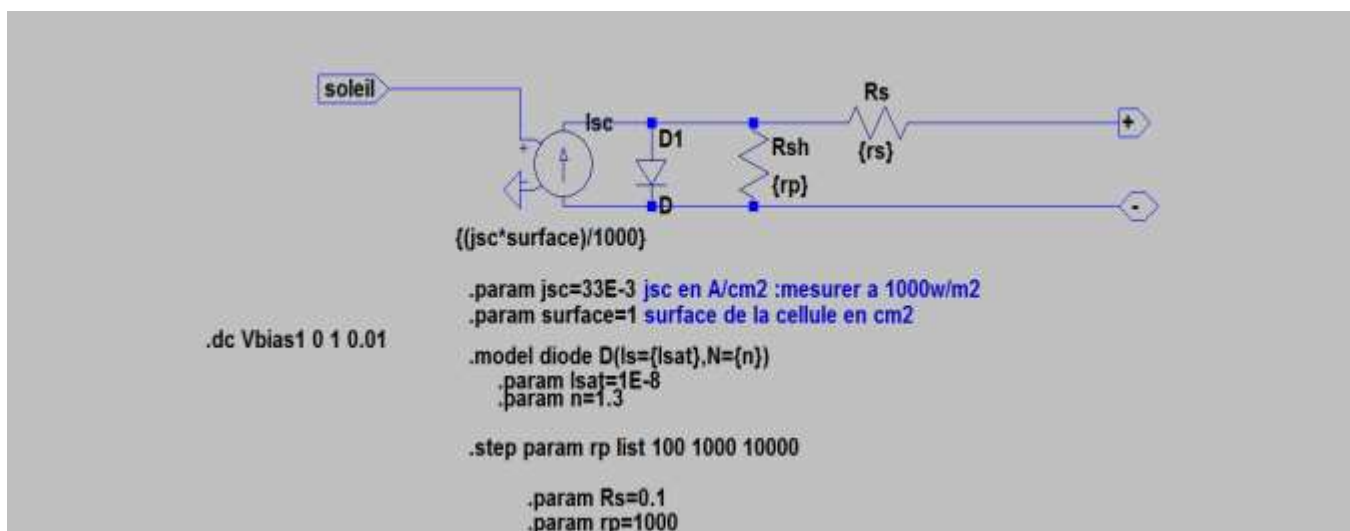
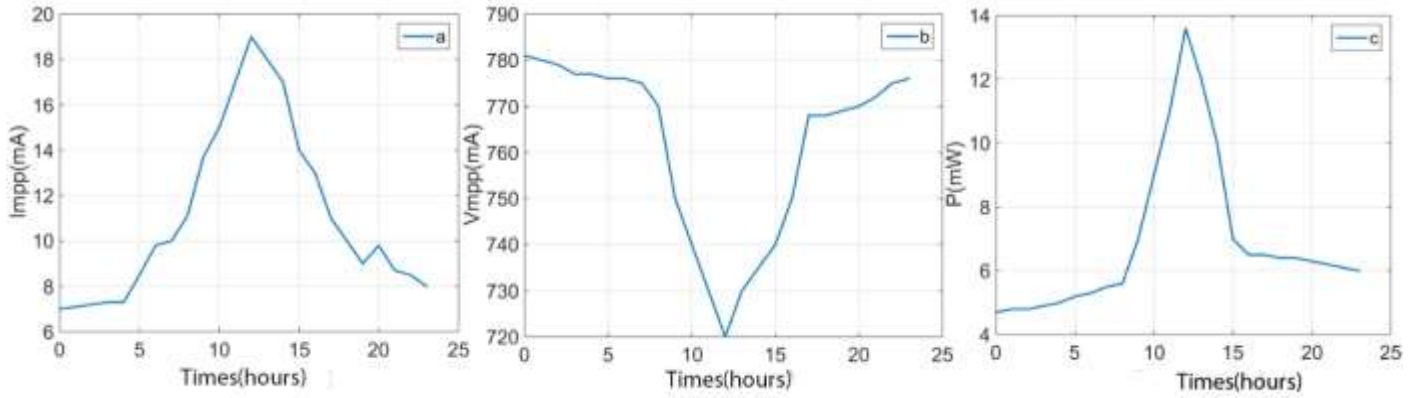**Figure 6.** Behavioral model of a photovoltaic cell.

Figure 7. Current voltage and power for beta equals.
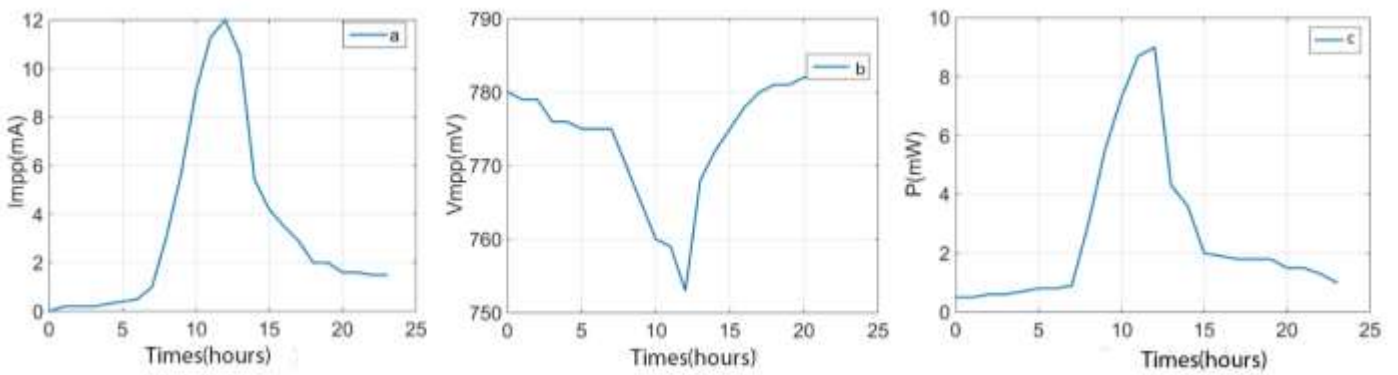

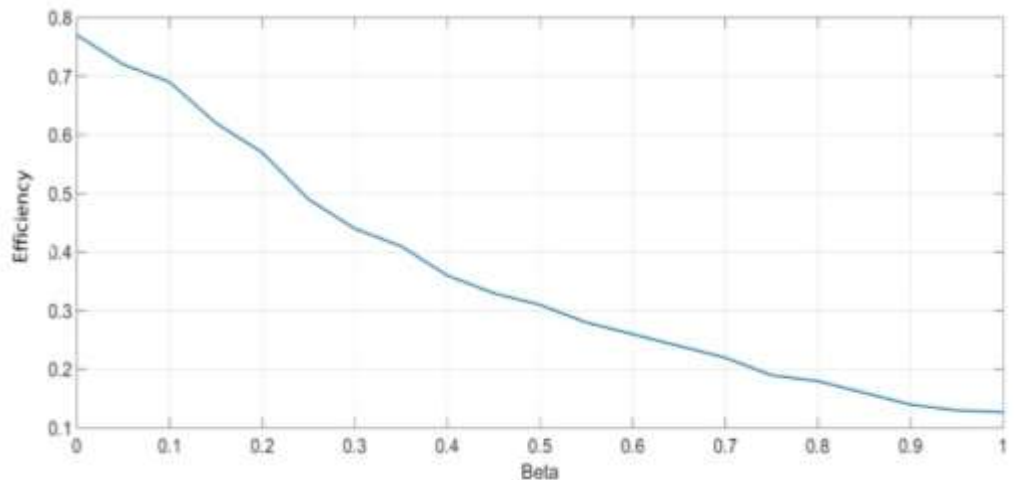**Figure 8.** Current voltage and power for beta equals 0.25.

Figure 9. Outcome variation as a function of beta.

atmosphere (Table 2).

We modelled a town of 40 houses, with an extension to 50 houses, 1 hydraulic pump, a mosque (Figure 10).

The solar energy potential of the area is provided by RESTSCREEN (Figures 11 and 12).

The energy needs of the town are estimated at 255.53

Table 2. Variation of photovoltaic cell as a function of aerosol amount in the environment.

Beta	0	0.05	0.1	0.15	0.2		0.25	
Functioning%	100	93.5	89.61	80.51	67.02		63.64	
Beta	3	3.35	0.4	0.45	0.5	0.55	0.6	
Functioning%	57.14	53.25	46.75	42.85	40.26	36.36	33.77	
Beta	0.65	0.7	0.75	0.8	0.85	0.9	0.95	1
Functioning%	31.17	28.51	24.67	23.37	20.78	18.18	16.89	16.50
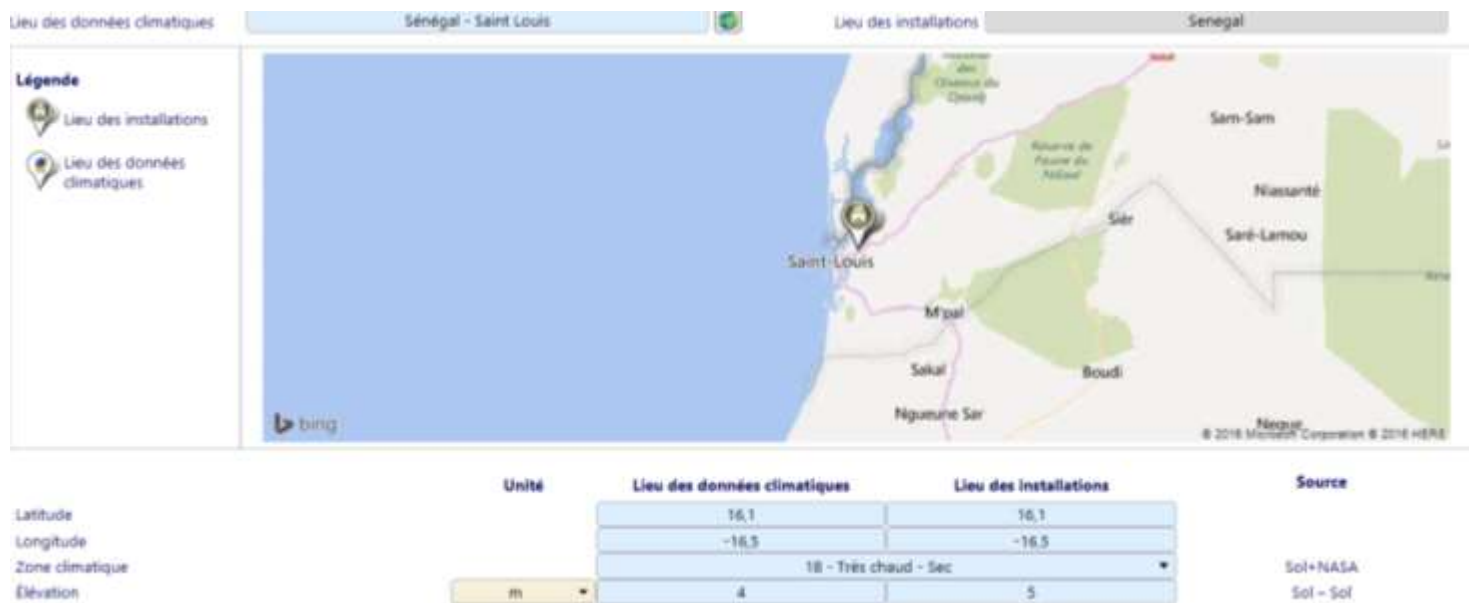
Figure 10. Ndiawdoun-Pont.

Figure 11. RESTScreen Saint Louis.

Figure 12. RESTScreen Saint Louis data.

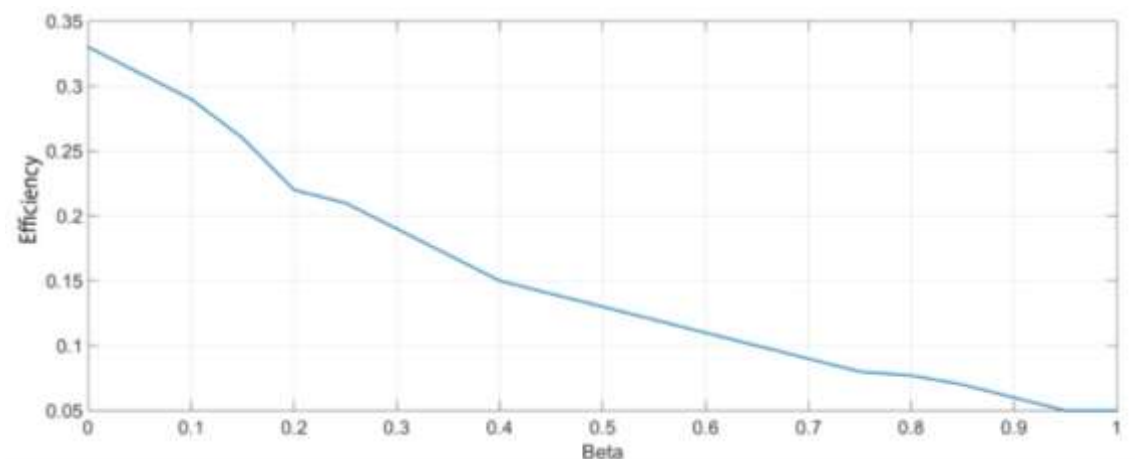| Mois	Température de l'air	Humidité relative	Précipitation	Rayonnement solaire quotidien - horizontal	Pression atmosphérique	Vitesse du vent	Température du sol	Degrés-jours de chauffage 18 °C	Degrés-jours de climatisation 10 °C
	°C	%	mm	kWh/m²/j	kPa	m/s	°C	°C-j	°C-j
Janvier	22,3	49,2%	3,72	4,97	101,3	3,9	24,9	0	381
Février	23,2	52,8%	1,67	5,48	101,2	4,3	26,9	0	370
Mars	23,7	59,1%	0,51	6,72	101,0	4,8	29,0	0	425
Avril	23,1	68,6%	0,41	7,27	100,9	5,3	31,4	0	393
Mai	23,9	72,2%	0,49	7,07	100,9	5,1	33,6	0	431
Juin	25,8	79,5%	4,89	6,34	101,0	4,5	34,1	0	474
Juillet	27,3	80,8%	35,87	6,28	101,1	4,3	33,1	0	536
Août	28,2	81,7%	101,76	6,24	101,0	3,8	32,0	0	564
Septembre	28,6	81,5%	84,81	5,80	101,0	3,3	32,2	0	558
Octobre	28,3	72,4%	21,56	5,67	101,0	3,4	33,5	0	567
Novembre	26,0	59,3%	1,26	5,04	101,1	3,5	30,8	0	480
Décembre	23,3	52,0%	1,40	4,72	101,2	3,5	26,8	0	412
Annuel	25,3	67,5%	258,35	5,97	101,1	4,1	30,7	0	5 592
Source	Sol	Sol	NASA	NASA	NASA	Sol	NASA	Sol	Sol
Mesuré à					m	10	0		

Données climatiques

Figure 13. Variation of photovoltaic field outcome as a function of aerosol amount in the environment.

KWh for a total power of 24.16 KW. The peak power (PC) required for the photovoltaic system is 71.34 KWp. The number of 250W / 24V panels required is 288.

The photovoltaic field outcome under optimal conditions, without aerosols, is 0.33.

By applying the photovoltaic cell operation to the photovoltaic field and considering the field as a much larger cell, we have the Figure 13 which expresses the variation of the photovoltaic field outcome as a function of beta.

Analyses and interpretations of the results

The results obtained allowed us to highlight the evolution of the irradiance compared to the atmospheric disorders, characterized by the Link factor, in which the Angström coefficient, which we called beta, is found.

Step 1

In Figure 4, we have the variation of the global daily radiation as a function of time for beta ranging from 0 to 1 in steps of 0.05. We are left with a "superposition of 21 curves" of different colors. Minimum was seen for each curve around 6 am and 6 pm; maximums around 12.

A difference of 645.5733 W / m2 between beta = 0 and beta = 1 is noted at the maximum overall radiated level (Figure 4). This difference shows the influence of the Angstrom coefficient in the radiative transfer.

The first results show the reduction of irradiance

according to the beta coefficient increase, which is nothing other than a Link Factor variable which gives us information on the quantity of aerosols in the atmosphere. This is consistent with the literature (DIOP 2012) because solar energy is attenuated (diffusion and absorption) by the presence of dust in the atmosphere.

Step 2

We modeled a CdTe cell on LTspace with the characteristics as shown in Figure 6. It is assigned the irradiation values obtained in "step 1". Note that the efficiency of cadmium telluride cell (CdTe) after simulation decreases. We go from an R (efficiency)> 0.7 to a R <0.2. The efficiency of the cell is affected by the presence of aerosols in the atmosphere. This is evidenced by the evolution of the maximum overall irradiation with respect to the Link factor.

The impact of aerosols on solar radiation results in lower cell efficiency. From the yields obtained, an operating mode of the photovoltaic sensor is obtained (Table 2) as a function of the Angstrom coefficient.

Step 3

The photovoltaic power plant that we have developed from a sizing of the village of Ndiawdoun-Pont provides for an atmosphere free of aerosols (beta = 0) a yield of 0.33 corresponding to a power of 71.34 KWc sufficient to supply Ndiawdoun-Pont.

By applying the operating mode (Table 2) to the photovoltaic field, considering the photovoltaic field as a macroscopic sensor, we observe:

For beta greater than 0 and less than 1 the yields are between 0.21 and 0.08. The plant operates less than 63.64%. This will impact the comfort of the village and concessions.
We have shown that atmospheric conditions impact photovoltaic production in the river region. The sunshine in the study area was made with an interactive beta coefficient. A characterization of the irradiation elaborated by modeling the radiation and a simulation of the yields of a photovoltaic power plant showed that there is a correlation between the output of the model and the renderings of the simulation.

The beta coefficient here makes it possible to determine the impact of aerosols on photovoltaic production in the area in question; the maximum sunshine rate of this zone is of the order of 127.2792 W/m^2 for beta equals 1. For low Beta we have a maximum of 772.825 W/m^2. This highlights the effect of aerosols. The link between the outputs of the irradiation model for two values of beta (1 and 0) when considering the maximums gives estimated yields at 0.05 and 0.33 of the photovoltaic plant subjected to a more or less disturbed by aerosols.

With known limit values it is possible to allow the informed population to make arrangements with regard to the devices consuming electrical energy at their disposal.

Conclusion and perspective

It is important to note that climate change will be one of the biggest environmental issues of the 21st century. Global warming impacts, which are visible over the past few years, demonstrate the urgent need for the international community to act in a concrete way for future generations and for countries vulnerable to climate change, and this by making the decrease as quickly as possible of greenhouse gases emissions.

Fossil energies are used abusively. Their transformation steps and their use raise a lot of environmental problems such as climate change with the phenomenon of global warming, which is the increase of temperatures over most of the oceans and the Earth's atmosphere, measured globally over several decades, and reflecting an increase heat retained on the earth's surface.

Senegal has a medial electrification level (Kande, 2018), with a good coverage in urban areas while it remains low in rural areas.

Thus, the issue raised is in relation with the improvement of people's living conditions by avoiding fossil fuels. The promotion and the use of renewable energies as well as photovoltaics are good solutions since we have an area with very strong sunlight.

The fact that photovoltaic technology uses solar radiation to produce energy is mentioned in this study. The atmosphere impacts affected by aerosols on radiation are also discussed in this study.

We highlighted the atmospheric conditions on photovoltaic production in the river area. An assessment of sunshine in the study area has been made. A characterization of the irradiation is elaborated by modelling the radiation and a simulation of photovoltaic power plant outcomes.
Based on the results obtained, we can estimate aerosols impact on photovoltaic production in the river area; we evaluated the sunshine rate of this zone through modelling. We chose an irradiation model to estimate the photovoltaic plant outcomes subjected to an atmosphere disturbed by aerosols.

Thanks to this work, it is possible to launch alerts and specific warnings to population benefiting from this type of resource concerning their consumption and their electricity consumption devices.

Perspective

On one hand, for a more effective alert model, we will have to consider the evolution of atmospheric conditions (clouds, rain). An advanced study of the factor of Link in the day, the month or even the season will refine the

recommendations and tips for the use of electrical devices powered by the plant.

On the other hand, the plant outcome will be better apprehended by considering meteorological parameters and aerosols deposit on the plant solar panels. The study will also continue on production and costs.

CONFLICT OF INTERESTS

The authors have not declared any conflict of interests.

REFERENCES

Dyer AJ, Hicks BB (1965). Measurement stratospherique transport of volcanic dust inferred from solar radiation. Nature 208(5006):131-133.

Abitan H, Bohr H, Buchhave P (2008). Correction to the Beer–Lambert–Bouguer law for optical absorption. Applied optics 47(29):5354-5357.

Arent D, Wise A, Gelman R (2011). The status and prospects of renewable energy for combating global warming. Energy Economics 33:584-593.

Bouhadda Y, Serri L (2006). Contribution à l'étude du trouble atmosphérique de Linke sur le site de Ghardaïa. Revue des Energies Renouvelables 9(4):277-284.

Chamani R, Monkam D, Djomou ZY (2018). Return times and return levels of July–September extreme rainfall over The Major Climatic Sub-Regions in Sahel. Atmospheric Research 212:77-90.

D'Almeida GA (1986). A model for saharan dust transport. Climate and Applied Meteorology 25:903-916.

Dickinson RE (1975). Solar variability and me lower atmosphere. Bulletin American Meteorological Society 56(12):1240-1248.

Diop B (2012). Etude énergétique de l'atmosphére à l'influence des lignes de grains dans la zone sahélienne. Ph.D. thesis. Cheikh Anta Diop University of Dakar. Sénégal.

Edouard M, Njom D (2013). Mathematical Modeling and Digital Simulation of PV Solar. International Journal of Emerging Technology and Advanced Engineering 3(9):24-32.

Gratzel M (2005). Solar Energy Conversion by Dye-Sensitized Photovoltaic Cells. Inorganic Chemistry 44(20):6841-6851.

Ineichen P (1992). Dynamic global-to-direct irradiance conversion models. ASHRAE Transactions 98(1):354-369.

Kaly F (2015). Variability of mineral dust concentrations overWest Africa monitored by the Sahelian Dust Transect. Atmospheric Research pp. 226-241.

Kande O (2018). Le soleil online. Retrieved 03 15 2018. From web site. http://www.lesoleil.sn/component/k2/item/76087-un-taux-d-electrification-rurale-de-40-en-2017.html

Kasten F (1996). The linke turbidity factor based on improved values of the integral rayleigh optical thickness. Solar Energy 56(3):239-244.

Laines-Canepa JR, Pina-Gutierrez JM, Azamar-Barrios JA, Sosa-Olivier JA, Ávila-Lázaro I (2017). Electric energy generation from a floating dome type biogas plant at a ranch in the southeast of Mexico. African Journal of Environmental Science and Technology pp. 361-369.

Maillard M (2017). Le Monde Afrique. Retrieved 02 10 2018 .From web site. https://www.lemonde.fr/afrique/article/2016/10/25/senergy-2-la-plus-grande-centrale-solaire-d-afrique-de-l-ouest-inauguree-au-senegal_5020110_3212.html

Martiny N, Roucou P, Pohl B, Camberlin P, Chiapello I (2016). Définition d'un événement de poussières désertiques au sahel : apport de nouvelles mesures de pm10 au burkina faso. XXVIIIe Colloque de l'Association Internationale de Climatologie. Liège.

Senghor H (2017). Étude de la variabilité spatio-temporelle et des processus contrôlant la distribution des aérosols désertiques en Afrique de l'Ouest et sur l'Atlantique tropical-est. Ph.D. thesis. Cheikh Anta Diop University of Dakar. Sénégal.